Avestia Publishing
Journal of Fluid Flow, Heat and Mass Transfer (JFFHMT)
Volume 11, Year 2024
ISSN: 2368-6111
DOI: 10.11159/jffhmt.2024.001

Design and Numerical Characterization of SAR $(Y\text{-}U)_H$ Micromixers

Md Readul Mahmud
Independent University, Bangladesh (IUB), Department of Physical Sciences
Plot 16 Block B, Aftabuddin Ahmed Road Bashundhara R/A, Dhaka-1229, Bangladesh
mahmud.readul@iub.edu.bd

Abstract - *A new micromixer named '$(Y\text{-}U)_H$' is proposed based on the split and recombine (SAR) principle. Five different $(Y\text{-}U)_H$ mixers are constructed with varying vertical cylindrical connector height H. The optimization is carried out by changing the height H from 0 mm to 0.8 mm at varying Reynolds numbers ranging from 1 to 100 using numerical simulation software Ansys 15. The numerical setup is validated by comparing the numerical data with the experimental results of a well-known SAR 'H' mixer. Proposed $(Y\text{-}U)_H$ mixers have superior mixing performance than the H mixer irrespective of Reynolds numbers. Furthermore, the $(Y\text{-}U)_H$ mixers show excellent efficiency ($\eta > 90\%$) at low Reynolds numbers ($Re \leq 1$). However, efficiency declines with the incline of Reynolds numbers due to the absence of secondary flow, and efficiency is about 64% for Reynolds numbers ranging from 10 to 100. Mixing efficiency also depends on the vertical cylindrical connector height (H); both efficiency and pressure drop increase with the increase of vertical cylindrical height. The $(Y\text{-}U)_{0.8\ mm}$ (H = 0.8 mm) mixer shows the highest maximum efficiency (74%) compared to all examined mixers.*

Keywords**:** CFD, Microfluidic, Micromixer, SAR.

© Copyright 2024 Authors - This is an Open Access article published under the Creative Commons Attribution License terms (http://creativecommons.org/licenses/by/3.0). Unrestricted use, distribution, and reproduction in any medium are permitted, provided the original work is properly cited.

1. Introduction

The field of microfluidics has attracted a lot of interest lately due to its many applications and quick progress [1]. Micromixers are tools used to combine fluids on a microscale, independent of their characteristics and nature, including density, viscosity, surface tension, etc. Numerous chemical processes, biological reactions, medication discovery and delivery, medical diagnostics, chemical synthesis, and the food sectors all make use of micromixers and microreactors [2], [3]. Rapid analysis, mobility, increased control, cheap cost, required less expensive chemicals, and excellent safety is some of the primary benefits of micromixers versus giant batch reactors or mixers [4], [5]. Other advantages of employing micromixers include their ease of manufacture, upkeep, and replacement, as well as their numerous biological uses, which range from medicine and drug delivery to the study of proteins and nucleic acids [6], [7]. Micromixers typically function at low Reynolds numbers (Re) resulting in primarily laminar flow. Therefore, the mixing mechanism is based on molecular diffusion, which necessitates a significant channel length and time to get optimal mixing performance [8]. Two different types of mixers—passive and active—are presented to address these drawbacks [9]. To improve the mixing process, active mixers take advantage of a variety of external energy sources, such as the magnetic, electric, temperature, acoustic, and periodic pressure fields, etc. [10], [11].

In contrast, passive mixers rely on unique physical characteristics, such as channel shape and size, to provide high performance even in the absence of an active element. Because active mixers need an additional energy source, are more complicated to fabricate, and are challenging to incorporate into microfluidic systems; they typically have better mixing efficiencies than passive ones [12]. Whereas passive mixers boost mixing quickly by using a herringbone wall, a grooved surface, barriers to the channel walls, baffles inside the channel, and divide and recombine (SAR) of the fluids, etc. [13].

Date Received: 2022-06-07
Date Revised: 2023-11-05
Date Accepted: 2024-01-03
Date Published: 2024-01-16

Fluids are continually separated and recombined in the SAR process, creating a variety of multi-laminations of fluids that greatly increase the contact surface area which in turn raises the mixing index [14], [15]. Numerous researchers have created and analyzed SAR mixers based on various ideas. Unbalance SAR mixer is proposed by authors [16], [17]; SAR mixer with obstacles or baffles is studied by authors [18]-[20], SAR mixer using curved channel designed by authors [21], [22] and SAR mixer designed with different shaped mixing unit [23], [24].

The fast expansion of computer memory and processing time has led to a rapid increase in the use of computational fluid dynamics (CFD) to analyze fluid dynamic properties. The computation of numerous parameters (pressure drop, velocity, efficiency, species concentration, etc.) and the thorough visualization of the mixing process and related flow patterns (streamlines, vortex formation, velocity vector, etc.) are made possible by numerical simulation [12]. Therefore, a large number of researchers are designing and analyzing innovative micromixers using CFD [25].

This study uses the SAR concept to create a novel passive micromixer, and it uses the commercial program Ansys FLUENT 15 to compute the mixing performance at different Reynolds numbers (*Re*). A '$(Y\text{-}U)_H$' mixer with four identical elements is proposed and by changing the vertical cylindrical channel lengths (H), the mixing performance is computed. As a comparison, the performance of a SAR 'H' mixer is also analyzed.

2. Micromixer Design

The SAR technique is utilized in the construction of a novel 3D passive micromixer called '$(Y\text{-}U)_H$' as shown in Figure 1. One 'Y' and one 'U' segment make up one element and four identical elements constitute the '$(Y\text{-}U)_H$' mixer. The cylindrical segments at the inlets and outlets have respective radii of 0.4 mm and 0.6 mm respectively.

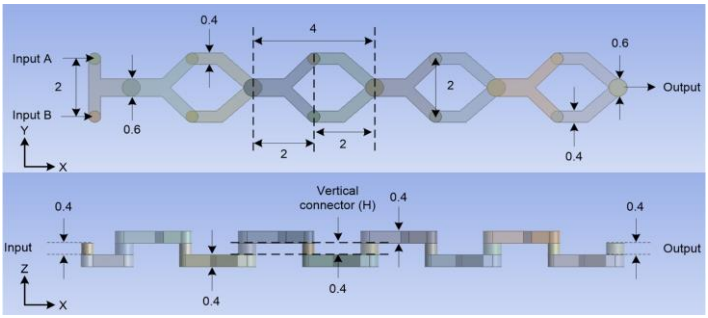

Figure 1. Diagram of the proposed $(Y\text{-}U)_H$ mixer (all the dimensions are in mm).

As represented in Figure 1, a vertical cylindrical connection (H) connects each element and each 'Y' and 'U' segment. The cylindrical connection (H) has a length that ranges from 0 mm to 0.8 mm, rising by 0.2 mm every step. Thus, $(Y\text{-}U)_{0\,mm}$ (H = 0 mm), $(Y\text{-}U)_{0.2\,mm}$ (H = 0.2 mm), $(Y\text{-}U)_{0.4\,mm}$ (H = 0.4 mm), $(Y\text{-}U)_{0.6\,mm}$ (H = 0.6 mm) and $(Y\text{-}U)_{0.8\,mm}$ (H = 0.8 mm) represent five '$(Y\text{-}U)_H$' mixers with various vertical connection heights.

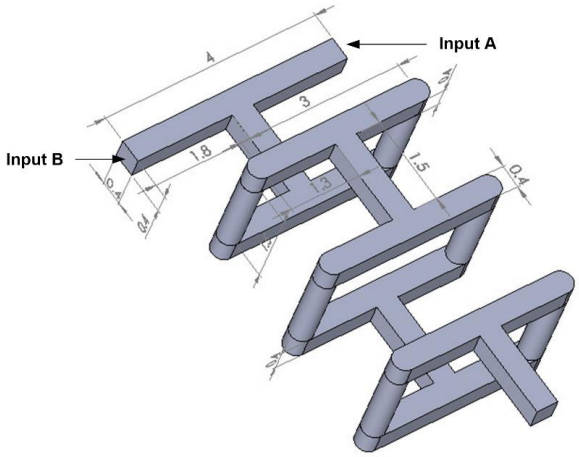

Figure 2. Diagram of H mixer (all the dimensions are in mm).

M. Nimafar et al. [26] have constructed and experimentally investigated the efficiency of the 'H' mixer for Reynolds numbers from 0.083 to 4.166. A newly designed H mixer is represented in Figure 2, the 'H' micromixer geometry is composed of two components: the straight channel and the H-segment, which denotes a single element. One element's length is 1.4 mm, while both inputs and outputs have widths and heights of 0.4 mm. The 'H' mixer has a total axial length of 20 mm and is made up of 12 identical elements (only 3 elements are shown below in Figure 2).

3. Numerical Method

Ansys FLUENT 15 uses the finite volume approach to study the mixer's flow characteristics and mixing performance. The mixed fluid leaves the mixer through the output after entering from two inputs. Both fluids in this investigation are assumed to have the physical characteristics of water. The density, viscosity, and diffusions constant of the water is $1000\,kg/m^3$, $0.001\,Pa\,s$ and $1\times10^{-9}\,m^2/s$, respectively. The following equation is used to determine the Reynolds numbers, which are a crucial quantity for fluid flow [27].

$$Re = \frac{\rho v d}{\mu} \quad (1)$$

Where ρ is the fluid density, μ is the dynamic viscosity, and v is the fluid velocity, evaluated at the rectangular channel. The characteristics length d equals 0.4 mm, which is the minimum dimension of the mixers.

An incompressible, laminar, Newtonian liquid in microchannels was taken into consideration. To discretize continuity, Navier-Stokes, and species convection-diffusion equations, Ansys FLUENT 15 used a coupled solver and finite volume approach [21], [28].

$$\nabla . V = 0 \quad (2)$$

$$\rho V . \nabla V = -\nabla P + \mu \nabla^2 \mathrm{V} \quad (3)$$

$$V . \nabla C = D \nabla^2 \mathrm{C} \quad (4)$$

Where P is equal to pressure, C is the mass concentration of the species, D is the coefficient of diffusion, and V is the fluid velocity vector. Additionally, ρ is the fluid density and μ is the fluid's dynamic viscosity. The diffusion constant used in this study is $1 \times 10^{-9}\, m^2/s$ which is a typical value for water-water mixing [13]. When the mass fraction of the two species reached 0.5, homogeneous mixing was accomplished. The mass concentration of the two species was set at 0 in Input A and 1 in Input B, respectively. No-slip boundary conditions were taken into consideration, and the inputs and output were configured as velocity inlet and pressure outlet, respectively. The implicit SIMPLEC method was utilized to integrate discrete equations linked in the pressure-velocity formulation.

The following formulas are used to determine the mixing performance, which serves as a common benchmark for assessing the mixing process [29] [30].

$$\sigma = \sqrt{\frac{1}{N} \cdot \sum_{i=1}^{N} (C_i - C_m)^2} \quad (5)$$

$$\eta = 1 - \sqrt{\frac{\sigma^2}{\sigma_{max}^2}} \quad (6)$$

Equations (5) and (6) use the following notation: σ stands for the mass fraction standard deviation at a cross-sectional plane; N is the number of data points in that cross-sectional plane; C_i is the mass fraction at a given point; C_m is the optimal mass fraction; σ_{max} is the maximum variance of the mass fraction over the data range; and η is the mixing efficiency, which swings between zero and one. For applications involving mixing processes, an efficiency of 80% to 100% is appropriate; zero denotes unmixed species and one indicates perfectly mixed species.

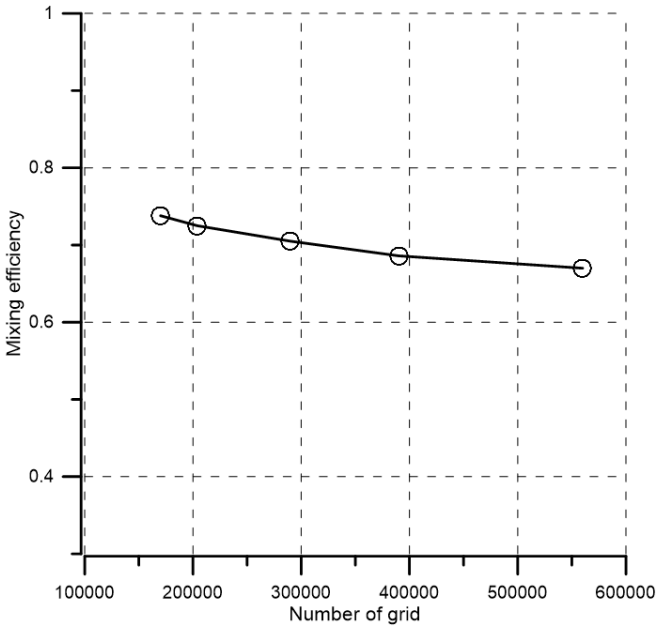

Figure 3. Mixing efficiency at the output of $(\text{Y-U})_{0.6\text{ mm}}$ mixer at $Re = 30$.

A high-quality mesh model is essential for accurate numerical results [31]. To make sure that numerical data are independent of grid size and shape, it is crucial to perform the mesh independence test [32]. Therefore, structured tetrahedral cells were employed for the numerical test [33]. A path-conforming technique was used to create tetrahedral grid networks without any suppression. For mixer $(\text{Y-U})_{0.6\text{ mm}}$ (H = 0.6 mm), six distinct grid systems with a range of nodes from 1.7×10^5 to 5.6×10^5 were investigated. Figure 3 displays the mixing efficiency for various grid numbers and there is a small variation in efficiency by increasing the number of grids at $Re = 30$. For the simulation, a grid system with 2.90×10^5 nodes were used in order to minimize the computational expense and time. For the remaining four $(\text{Y-U})_{\text{H}}$ mixers, a grid dependency test was also conducted, and nodes of 2.72×10^5, 2.76×10^5, 2.98×10^5, and 2.94×10^5 were selected for $(\text{Y-U})_{0\text{ mm}}$, $(\text{Y-U})_{0.2\text{ mm}}$, $(\text{Y-U})_{0.4\text{ mm}}$ and $(\text{Y-U})_{0.8\text{ mm}}$ mixers, respectively.

4. Result and Discussion

A SAR "H" mixer [26] was created, and numerical simulations for $0.083 \leq Re \leq 4.166$ were run in order to validate the numerical approach. Figure 4 illustrates a comparison between the numerical data of present study and published experimental data for the H mixer after 20 mm along axial length. The agreement between experimental data and numerical simulation findings is good, with less than a 10% deviation.

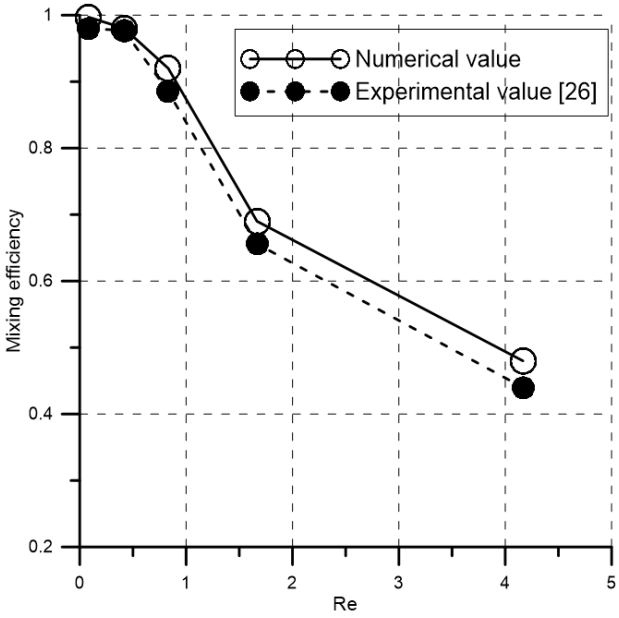

Figure 4. Experimental mixing efficiency of H mixer reported by M. Nimafar et al. [26] and numerical mixing efficiency in the present study.

Figure 5 shows the comparison of pressure drop and numerical mixing efficiency between the $(Y\text{-}U)_{0\ mm}$ mixer and the H mixer. It is clear that, for all Reynolds numbers considered, the $(Y\text{-}U)_{0\ mm}$ mixer not only has better efficiency but also a smaller pressure drop than the H mixer. At $Re = 100$, the $(Y\text{-}U)_{0\ mm}$ mixer produces five times less pressure drop (400 Pa), and three times higher efficiency (64%) compared to the H mixer. It follows that, for all Reynolds values considered, the suggested $(Y\text{-}U)_{0\ mm}$ mixer outperforms the H mixer. As a result, only $(Y\text{-}U)_{H}$ mixers were examined in further detail.

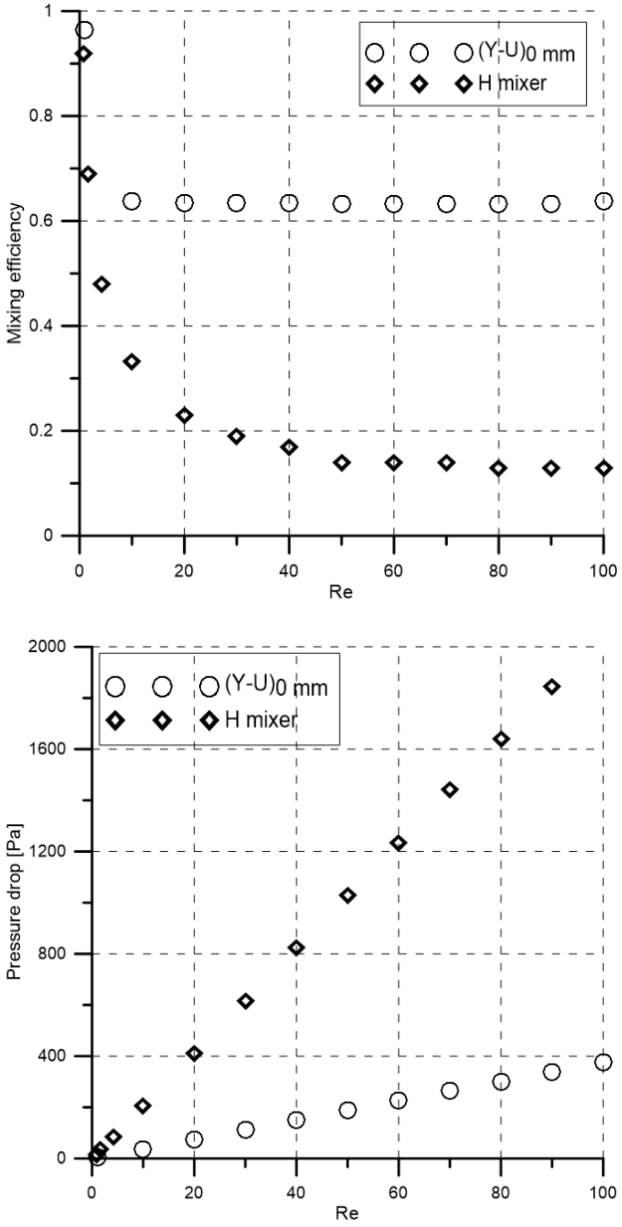

Figure 5. Efficiency (top) and pressure drop (down) of $(Y\text{-}U)_{0\ mm}$ and H mixers.

The overall mixing performance of all mixers with different vertical connector height H (0 mm to 0.8 mm) was analyzed. Figure 6 displays the water mass fraction inside the mixers at Reynolds numbers equal to 1 and 50. At $Re = 50$ there is a large fluctuation in the water mass fraction for every mixer. Water concentration changes noticeably as Reynolds numbers rise from 1 to 50, indicating that efficiency would decline at high Reynolds numbers ($Re = 50$) in comparison to low Re ($Re = 1$).

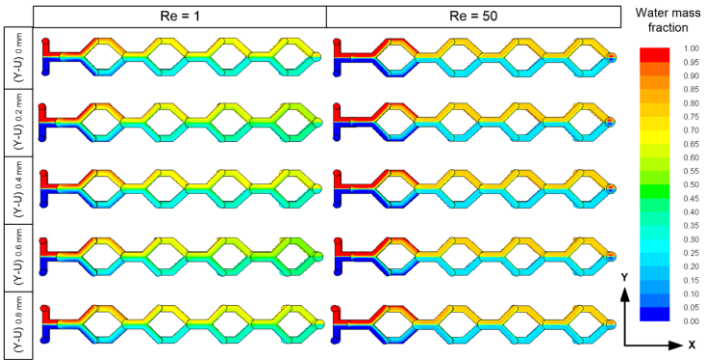

Figure 6. Distribution of water mass fraction of $(Y\text{-}U)_H$ mixers on the XY-plane.

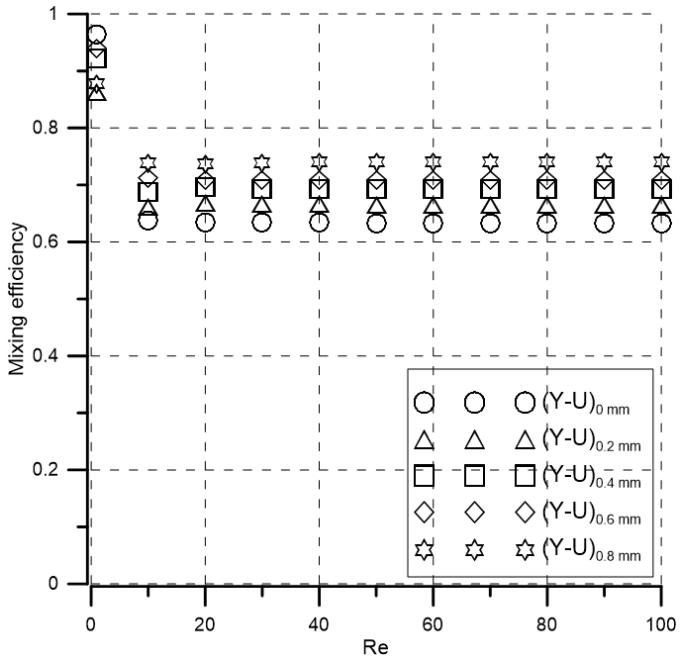

Figure 7. Mixing efficiency of $(Y\text{-}U)_H$ mixers at varying Reynolds numbers.

Figure 7 shows the variation curves of mixing efficiency (η) for $(Y\text{-}U)_H$ micromixers changing the vertical cylindrical connecting height (H) under different Reynolds numbers. It can be found that all mixers show the same trend at Reynolds numbers ranging from 1 to 100. At low Reynolds numbers ($Re = 1$), the liquid flows at a low speed in the channel, and the mixing mechanism is mainly diffusion. Hence good mixing is achieved due to longer residence time, which is about 90% for all mixers. As the Re value increases, the flow rate in the mixer increases, and the time for the diffusion of chemical molecules decreases, resulting in a decrease in the mixing efficiency. When ($Re \geq 10$), the mixing index do not changes with the increase of Re, influence of the secondary flow is not strong enough to compensate for the shorter mixing time due to the increase in flow rate (as shown in Figure 8). It is clear that mixing efficiency depends positively on vertical connector height (H). Efficiency increases with the increase of H because of extra path length which in turn gives additional mixing time. All mixers exceed 60% efficiency at higher Reynolds numbers ($10 \leq Re \leq 100$). Moreover, $(Y\text{-}U)_{0.8\ mm}$ yields the highest efficiency (74%) for $10 \leq Re \leq 100$.

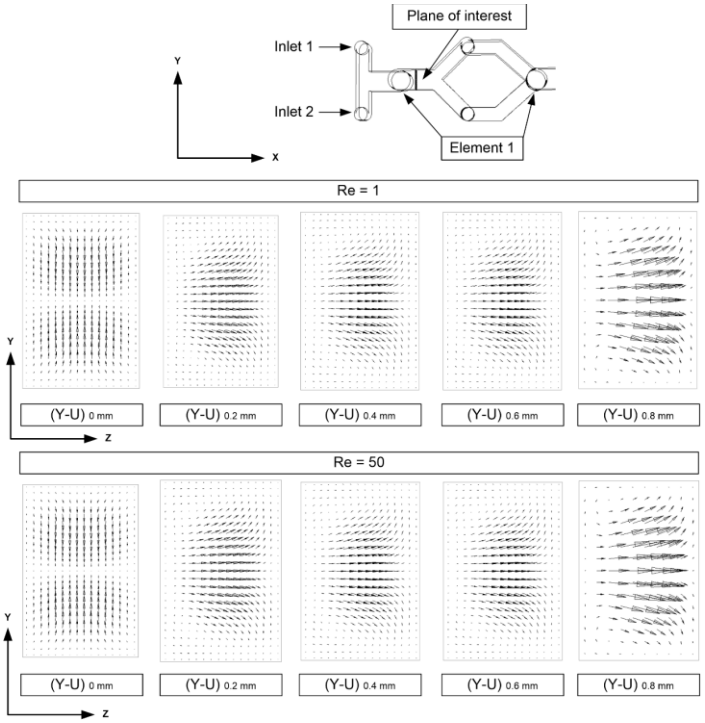

Figure 8. The velocity vector of $(Y\text{-}U)_H$ mixers on the YZ-plane at $Re = 1$ and $Re = 50$.

Figure 8 depicts the velocity vector plots on the YZ-plane for five mixer channels at $Re = 1$ and $Re = 50$. The flow pattern is almost the same in every cross-section, and the secondary flow is negligible. But the efficiency is good because at low Reynolds numbers ($Re = 1$) fluids have more time to mix. At a Reynolds number of 50, the secondary flow increases for all mixers but not at a significant level. Hence the efficiency decreases at high Reynolds numbers ($10 \leq Re \leq 100$).

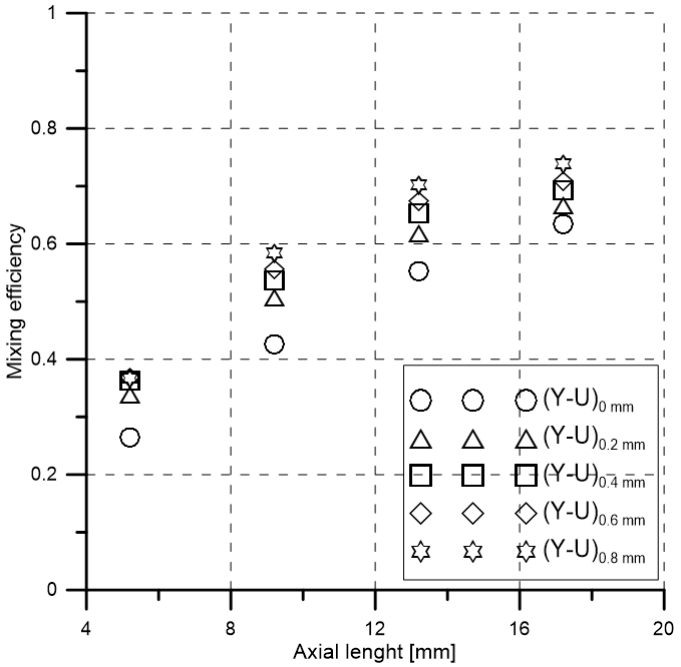

Figure 9. Mixing efficiency of $(Y\text{-}U)_H$ mixers along the axial length at $Re = 30$.

The relationship between mixing efficiency and axial length at $Re = 30$ is presented in Figure 9. The curves follow the same trend and efficiency increases with the axial length, as expected. The $(Y\text{-}U)_{0\ mm}$ mixer shows the lowest efficiency, and the $(Y\text{-}U)_{0.8\ mm}$ mixer shows the highest efficiency (74%) at the output due to its longer fluid path. An efficiency of more than 95% can be reached by adding more elements which will increase the total fluid path.

Figure 10 expresses the relationship between pressure drop, flow rate, and Reynolds numbers varying from 1 to 100. Pressure drops increase with the increase of Reynolds numbers (and flow rate) for all mixers. It is evident that vertical cylindrical connecting height (H) affects the pressure drop; pressure drop increases with the increase of vertical cylindrical connecting height (H). The $(Y\text{-}U)_{0.8}$ (H = 0.8 mm) mixer has the highest pressure drop due to its longest channel length.

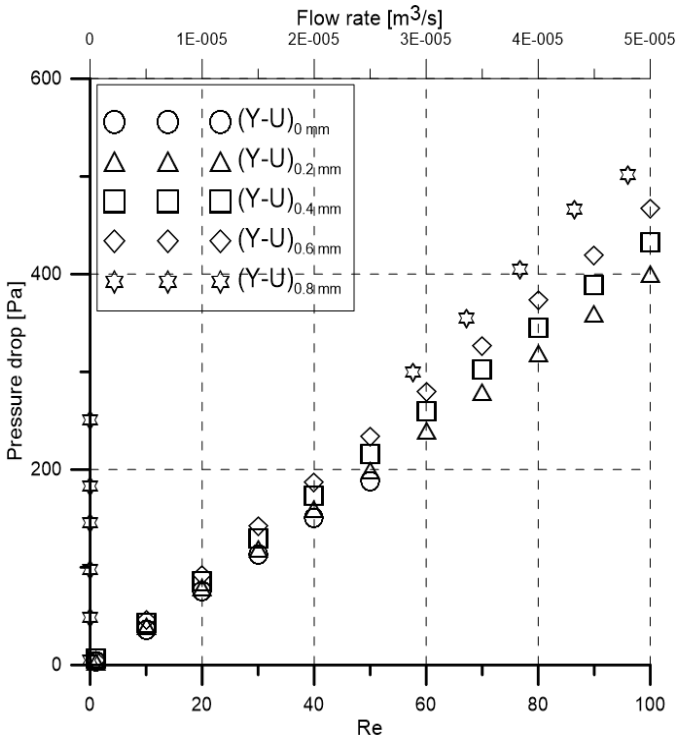

Figure 10. Pressure drop of the $(Y\text{-}U)_H$ mixers at varying Reynolds numbers and Flow rates.

6. Conclusion

The design and investigation of the performance of novel SAR $(Y\text{-}U)_H$ mixers are the main purposes of this work. A $(Y\text{-}U)_H$ mixer is made up of four identical elements. The vertical connecting cylindrical length (H) of the mixer is changed from 0 mm to 0.8 mm by 0.2 mm each time to observe the impact on the mixing index. Using Ansys FLUENT 15 mixing performance is estimated numerically changing Reynolds numbers ($1 \leq Re \leq 100$). Additionally, a well-known SAR 'H' mixer is examined, and the numerical data is computed and compared with published experimental data. At all investigated Reynolds numbers, the suggested $(Y\text{-}U)_H$ mixers perform better than the existing H mixer. The $(Y\text{-}U)_{0.8\ mm}$ mixer offers the best mixing efficiency (74%) compared to all proposed mixers. Since secondary flow is not strongly present in the mixers, increasing Reynolds numbers does not result in an improvement in mixing efficiency. However, because the fluids have adequate time to mix, efficiency is high (90%) for low Reynolds numbers ($Re = 1$). Therefore, the $(Y\text{-}U)_H$ mixers have potential applications at low Reynolds numbers.

References

[1] D. Wang, D. Ba, K. Liu, M. Hao, Y. Gao, Z. Wu and Q. Mei, "A Numerical Research of Herringbone Passive Mixer at Low Reynold Number Regime," *Micromachines*, vol. *8*, pp. 325, 2017. doi: 10.3390/mi8110325

[2] V. Khaydarov, E. S. Borovinskaya and W. Reschetilowski, "Numerical and Experimental Investigations of a Micromixer with Chicane Mixing Geometry," *Appl. Sci.* vol. *8*, pp. 2458, 2018. doi.org/10.3390/app8122458

[3] C. Y. Lee, W. T. Wang, C. C. Liu and L. M. Fu, "Passive mixers in microfluidic systems: A review," *Chemical Engineering Journal*, vol. 288. pp. 146–160, 2016. doi: 10.1016/j.cej.2015.10.122

[4] S. Rampalli, T. M. Dundi, S. Chandrasekhar, V. R. K. Raju and V. P. Chandramohan, "Numerical Evaluation of Liquid Mixing in a Serpentine Square Convergent-divergent Passive Micromixer," *Chem. Prod. Process Model.*, vol. 15, no. 2, pp. 1–11, 20203 doi: 10.1515/cppm-2019-0071

[5] G. Cai, L. Xue, H. Zhang and J. Lin, "A review on micromixers," *Micromachines*, vol. 8, no. 9, 2017. doi: 10.3390/mi8090274

[6] A. Enders, I. G. Siller, K. Urmann, M. R. Hoffmann and J. Bahnemann, "3D Printed Microfluidic Mixers—A Comparative Study on Mixing Unit Performances," *Small*, vol. 15, no. 2, 2019. doi: 10.1002/smll.201804326

[7] N. T. Nguyen and Z. Wu, "Micromixers - A review," *Journal of Micromechanics and Microengineering*, vol. 15, no. 2. 2005. doi: 10.1088/0960-1317/15/2/R01

[8] M. Guo, X. Hu, F. Yang, S. Jiao, Y. Wang, H. Zhao, G. Luo and H. YuM, "Mixing Performance and Application of a Three-Dimensional Serpentine Microchannel Reactor with a Periodic Vortex-Inducing Structure," *Ind. Eng. Chem. Res.*, vol. 58, no. 29, pp. 13357–13365, 2019. doi: 10.1021/acs.iecr.9b01573

[9] M. R. Mahmud, S. Hossain and J. H. Kim, "A SAR Micromixer for Water-Water Mixing: Design, Optimization, and Analysis," *Process*, vol. 9, pp. 1926, 2021. doi: 10.3390/PR9111926

[10] V. Khaydarov, E. S. Borovinskaya, and W. Reschetilowski, "Numerical and experimental investigations of a micromixer with chicane mixing geometry," *Appl. Sci.*, vol. 8, no. 12, pp. 3–6, 2018. doi: 10.3390/app8122458

[11] A. Usefian and M. Bayareh, "Numerical and experimental investigation of an efficient convergent–divergent micromixer," *Meccanica*, vol. 55, no. 5, pp. 1025–1035, 2020. doi: 10.1007/s11012-020-01142-0

[12] M. Juraeva and D. J. Kang, "Mixing performance of a cross-channel split-and-recombine micro-mixer combined with mixing cell," *Micromachines*, vol. 11, no. 7, 2020. doi: 10.3390/mi11070685

[13] V. Viktorov, M. R. Mahmud, and C. Visconte, "Design and characterization of a new H-C passive micromixer up to Reynolds number 100," *Chem. Eng. Res. Des.*, vol. 108, pp. 152–163, 2016. doi: 10.1016/j.cherd.2015.12.005

[14] V. Viktorov and M. Nimafar, "A novel generation of 3D SAR-based passive micromixer: Efficient mixing and low-pressure drop at a low Reynolds number," *J. Micromechanics Microengineering*, vol. 23, no. 5, 2013. doi: 10.1088/0960-1317/23/5/055023

[15] V. Viktorov, C. Visconte, and M. R. Mahmud, "Analysis of a Novel Y-Y Micromixer for Mixing at a Wide Range of Reynolds Numbers," *J. Fluids Eng. Trans.*, vol. 138, no. 9, pp. 1–9, 2016. doi: 10.1115/1.4033113

[16] M. A. Ansari, K. Y. Kim, K. Anwar, and S. M. Kim, "A novel passive micromixer based on unbalanced splits and collisions of fluid streams," *J. Micromechanics Microengineering*, vol. 20, no. 5, 2010. doi: 10.1088/0960-1317/20/5/055007

[17] S. Hossain and K. Y. Kim, "Mixing analysis of passive micromixer with unbalanced three-split rhombic sub-channels," *Micromachines*, vol. 5, no. 4, pp. 913–928, 2014. doi: 10.3390/mi5040913.

[18] W. Raza and K. Y. Kim, "Asymmetrical split-and-recombine micromixer with baffles," *Micromachines*, vol. 10, no. 12, 2019. doi: 10.3390/mi10120844

[19] S. W. Lee and S. S. Lee, "Rotation effect in split and recombination micromixing," *Sensors Actuators, B Chem.*, vol. 129, no. 1, pp. 364–371, 2008. doi: 10.1016/j.snb.2007.08.038

[20] M. R. Mahmud, "Numerical Analysis of a Planar O Micromixer with Obstacles," *J. Eng. Adv.*, vol. 3, no 2, pp 64-71, 2022. doi.org/10.38032/jea.2022.02.004

[21] T. S. Sheu, S. J. Chen and J. J. Chen, "Mixing of a split and recombine micromixer with tapered curved microchannels," *Chem. Eng. Sci.*, vol. 71, pp. 321–332, 2012. doi: 10.1016/j.ces.2011.12.042

[22] G. Xia, J. Li, X. Tian and M. Zhou, "Analysis of flow and mixing characteristics of planar asymmetric split-and-recombine (P-SAR) micromixers with fan-shaped cavities," *Ind. Eng. Chem. Res.*, vol. 51, no. 22, pp. 7816–7827, 2012. doi: 10.1021/ie2026234

[23] S. Hardt, H. Pennemann, and F. Schönfeld, "Theoretical and experimental characterization of a

low-Reynolds number split-and-recombine mixer," *Microfluid. Nanofluidics*, vol. 2, no. 3, pp. 237–248, 2006. doi: 10.1007/s10404-005-0071-6

[24] D. S. Kim, S. H. Lee, T. H. Kwon and C. H. Ahn, "A serpentine laminating micromixer combining splitting/recombination and advection," *Lab Chip*, vol. 5, no. 7, pp. 739–747, 2005. doi: 10.1039/b418314b

[25] G. Orsi, M. Roudgar, E. Brunazzi, C. Galletti and R. Mauri, "Water-ethanol mixing in T-shaped microdevices," *Chem. Eng. Sci.*, vol. 95, pp. 174–183, 2013. doi: 10.1016/j.ces.2013.03.015

[26] M. Nimafar, V. Viktorov and M. Martinelli, "Experimental comparative mixing performance of passive micromixers with H-shaped sub-channels," *Chem. Eng. Sci.*, vol. 76, pp. 37–44, 2012. doi: 10.1016/j.ces.2012.03.036.

[27] M. Nimafar, V. Viktorov and M. Martinelli, "Experimental Investigation of Split and Recombination Micromixer in Confront with Basic T- and O- type Micromixers," *International Journal of Mechanics and Applications*, vol. 2, no. 5, pp. 61–69, 2012. DOI: 10.5923/j.mechanics.20120205.02

[28] J. M. Park, D. S. Kim, T. G. Kang and T. H. Kwon, "Improved serpentine laminating micromixer with enhanced local advection," *Microfluid. Nanofluidics*, vol. 4, no. 6, pp. 513–523, 2008. doi: 10.1007/s10404-007-0208-x

[29] W. Raza, S. Hossain and K. Y. Kim, "A review of passive micromixers with a comparative analysis," *Micromachines*, vol. 11, no. 5, 2020. doi: 10.3390/MI11050455

[30] M. R. Mahmud, "Numerical Investigation of Liquid–Liquid Mixing in Modified T Mixer with 3D Obstacles," *J. Eng. Adv.*, vol. 2, no. 2, pp 87-94, 2021. doi.org/10.38032/jea.2021.02.004

[31] C. K. Chung and T. R. Shih, "A rhombic micromixer with asymmetrical flow for enhancing mixing," *J. Micromechanics Microengineering*, vol. 17, no. 12, pp. 2495–2504, 2007. doi: 10.1088/0960-1317/17/12/016

[32] X. Shi, L. Wang, S. Huang and F. Li, "A novel passive micromixer with an array of Koch fractal obstacles in a microchannel," *J. Dispers. Sci. Technol.*, vol. 42, no. 2, pp. 236–247, 2021. doi: 10.1080/01932691.2019.1674156

[33] T. Dehghani, F. Sadegh Moghanlou, M. Vajdi, M. Shahedi Asl, M. Shokouhimehr and M. Mohammadi, "Mixing enhancement through a micromixer using topology optimization," *Chem. Eng. Res. Des.*, vol. 161, pp. 187–196, 2020. doi: 10.1016/j.cherd.2020.07.008